Thermal Stability and Emissivity Behavior (7-14 μm) of Ca-Sulfides under Simulated Daytime Surface Conditions for Multiple Mercury days: Implications for the formation of hollows and CaS detection by MERTIS onboard the BepiColombo mission

Indhu Varatharajan[1,2], Claudia Stangarone[1], Sergio Speziale[3], Alessandro Maturilli[1], Jörn Helbert[1], Harald Hiesinger[4], Iris Weber[4], Karin E. Bauch[4]

[1]Department of Planetary Laboratories, Institute of Planetary Research, German Aerospace Center (DLR), Berlin, Germany.

[2]Institute of Geological Sciences, Freie University (FU) Berlin, Germany.

[3]Helmholtz Centre Potsdam - GFZ German Research Centre for Geosciences, Potsdam, Germany.

[4]Institut für Planetologie, Westfälische Wilhelms-Universität Münster, Germany

Highlights

1. Spectral emissivity behavior (7-14 μm) of calcium-sulfides (CaS) remains stable for repeated heating cycles under simulated Mercury daytime surface conditions.
2. CaS is the stable sulfide that survives the extreme thermal environment of Mercury.
3. CaS is an important tracer for other sulfides those might be lost in the hollow-forming process dominated by sublimation.

Abstract

Global mapping of the nature and distribution of volatiles such as sulfides on Mercury's surface is essential for understanding the thermal evolution of the planet. The surface exposure of these sulfides over extreme day-night temperature cycles (176 days; 450 °C to -170 °C) on Mercury leads to thermal weathering of these sulfide compounds. It has been seen that among the proposed sulfides on Mercury (MgS, FeS, CaS, CrS, TiS, NaS, and MnS), CaS showed relatively stable and distinctive spectral features in the thermal infrared region (TIR; 7-14 μm) when studied under the simulated Mercury day conditions for temperatures ranging from 100 °C up to 500 °C under vacuum (0.1 mbar) (Varatharajan et al., 2019). In this study, we re-investigated the stability of CaS and its spectral emissivity spectral behavior. We exposed the sample for four consecutive Earth days simulating Mercury day cycles and measured the TIR spectra of CaS for temperatures up to 500 °C (with steps of 100 °C) every day. This time the spectral analysis is coupled and supported by XRD diffraction on the fresh and temperature-processed sample, showing the mineralogical evolution with temperature. We confirm that CaS is a stable compound and therefore it would remain stable on Mercury's surface regardless of investigated peak surface temperatures. This study further implies that, for the hollows dominated by the sublimation of sulfides on Mercury (Blewett et al., 2013; Helbert et al., 2013a; Vilas et al., 2016), CaS could be the last of the sulfides that could be mapped on Mercury as other sulfides were lost by thermal decomposition, leaving behind hollows. This could make CaS an important tracer for other sulfides, which might be lost in the hollow-forming process and supports the detection of CaS within hollows by MESSENGER (Vilas et al., 2016). The emissivity spectra reported here are significant for the detection and mapping of CaS

associated with hollows and pyroclastics using the Mercury Radiometer and Thermal Imaging Spectrometer (MERTIS) datasets.

Keywords: Mercury; Thermal Weathering; Emissivity; Spectroscopy; CaS; Hollows

1 Introduction

NASA's MESSENGER (Mercury Surface, Space Environment, Geochemistry, and Ranging) mission revealed that Mercury, unlike the Moon, has been formed in a highly reducing environment with sulfur abundances of up to 4 wt% (Nittler et al., 2011). MESSENGER's XRS (X-Ray Spectrometer) data suggest that FeS and CaS are present in Mercury's shallow regolith, with minor MnS and $NaCrS_2$ (Nittler et al., 2011; Weider et al., 2016). Thermochemical and experimental evidence indicates that CaS is the major lithophile sulfide on Mercury (Vaughan, 2013), supported by MESSENGER XRS data, which showed a strong correlation in the detected abundances of Ca and S, suggesting the presence of minerals such as oldhamites (Nittler et al., 2011; Weider et al., 2016; Weider et al., 2014; Weider et al., 2012). Sulfides have been proposed to be present at unique sub-km scale landforms called hollows (Helbert et al., 2013a). This hypothesis has been supported by the first spectral evidence of sulfide minerals (CaS, MgS) within the hollows of Dominici crater detected by MESSENGER Mercury Dual-Imaging System (MDIS) that mapped Mercury's surface in the visible-infrared spectral region (400 to 1000 nm) (Vilas et al., 2016). The global spectral mapping of identified hollows and pyroclastics utilizing at wide spectral ranges will enable us to effectively map the sulfide materials across Mercury's surface (Besse et al., 2020; Helbert et al., 2013a; Lucchetti et al., 2018; Thomas et al., 2014a, b; Vilas et al., 2016).

The Mercury Radiometer and Thermal Imaging Spectrometer (MERTIS) onboard the Mercury Planetary Orbiter (MPO) of ESA/JAXA's BepiColombo mission

will be the first orbital thermal infrared spectrometer (TIS) and radiometer (TIR) to map the surface mineralogy in the mid-infrared spectral range (Hiesinger et al., 2020; Hiesinger et al., 2010). With its two channels (TIS, TIR), MERTIS will characterize the emissivity behavior of surface materials, including sulfides, between 7 μm and 14 μm (TIS) (between 7 μm and 40 μm with TIR) with a spectral resolution of 90 nm (78 spectral channels) and a spatial resolution of 500m/pixel along with its corresponding surface temperature.

In a recent study (Varatharajan et al., 2019), the emissivity behavior of a wide range of sulfides (MgS, FeS, CaS, CrS, TiS, NaS, and MnS) within the MERTIS spectral range (7-14μm) were studied for temperatures ranging from 100 °C up to 500 °C, with heating steps of 100 °C under vacuum (0.1 mbar). The study showed that, among these sulfides, only CaS exhibited strong emissivity features and minor susceptibility to thermal weathering while reaching extreme temperatures of 500 °C for one simulated Mercury day (Varatharajan et al., 2019).

Mercury's surface is repeatedly exposed to extreme temperature changes, ranging from 450 °C during daytime to -170 °C during nighttime over a one day/night cycle of 176 terrestrial days (Krotikov and Shchuko, 1975; Soter and Ulrichs, 1967). In this study, we aim at further investigating the physical/thermal and emissivity/spectral stability of CaS while exposed to an extreme thermal environment for multiple simulated Mercury days as a function of temperature (100 °C, 200 °C, 300 °C, 400 °C, and 500 °C) under vacuum (0.1 mbar) for each day (see Section 2.1). For the whole duration of the experiment, the vacuum was maintained inside the emissivity chamber. The physical stability of CaS is studied by X-Ray diffraction (XRD) analysis of the starting (fresh synthetic) CaS and the resulting thermally processed CaS after four simulated Mercury days (Section 2.2). Our study is important for understanding the

thermal stability of the volatile-bearing materials such as CaS under Mercury daytime surface conditions for their effective detection from the orbit by MERTIS.

2. Sample, Facility and Methods

For this study, the starting material used is synthetic CaS with a grain size of ~10 μm (certified by industrial supplier Alfa Aesar; CAS No. 20548-54-3) as used in the study by (Varatharajan et al., 2019). The facility and methods for emissivity and x-ray diffraction studies are explained below in sections 2.1 and 2.2 respectively.

2.1 Emissivity

Planetary Spectroscopy Laboratory (PSL) is located at the Institute of Planetary Research, German Aerospace Center (DLR) in Berlin, Germany. Among the facilities present at PSL, the emissivity chamber allows to heat up various analogue materials, reaching extreme temperatures and to study their emissivity behaviors as a function of temperature (50 °C-600 °C) across a wide spectral range (1-50 μm). The systematic emissivity studies results in an extensive planetary materials emissivity library. Such specialized spectral library is created to support surface composition analyses of hot planetary targets such as Mercury, Venus, Moon, and Io (Helbert et al., 2019; Helbert and Maturilli, 2009; Helbert et al., 2013a; Helbert et al., 2013b; Maturilli et al., 2008; Varatharajan et al., 2019). One of the three identical FTIR (Fourier transform infrared) spectrometers (Bruker Vertex 80V) at PSL is connected to the external emissivity chamber (Fig. 1). The spectrometer is optimized for spectral measurements under vacuum conditions (0.1 mbar). The chamber is separated from the spectrometer by a shutter and a vacuum-tight optical window between the chamber and the spectrometer, enabling the chamber to be operated under vacuum or at the desired pressure condition.

For this study, the fresh CaS sample is placed in a stainless-steel cup which is then placed on a carousel, that can be rotated via a stepper motor to bring several samples to the measurement position without breaking the vacuum inside the chamber. The sample is heated from below the carousel (made of quartz glass) by an induction system. The temperature of the sample cup is controlled by adjusting the current applied to the induction coil. Three temperature sensors (thermopiles) on the sample and on the side of the sample cup, continuously monitor the bulk surface temperature, while the surrounding environment of the sample is monitored by a webcam (Fig. 1). The spectrometer is equipped with MCT HgCdTe detector (cooled by liquid nitrogen) and KBr beamsplitter to study the emissivity behavior of CaS at the TIR spectral region (7-14 μm) at the spectral resolution of 4 cm^{-1} under vacuum.

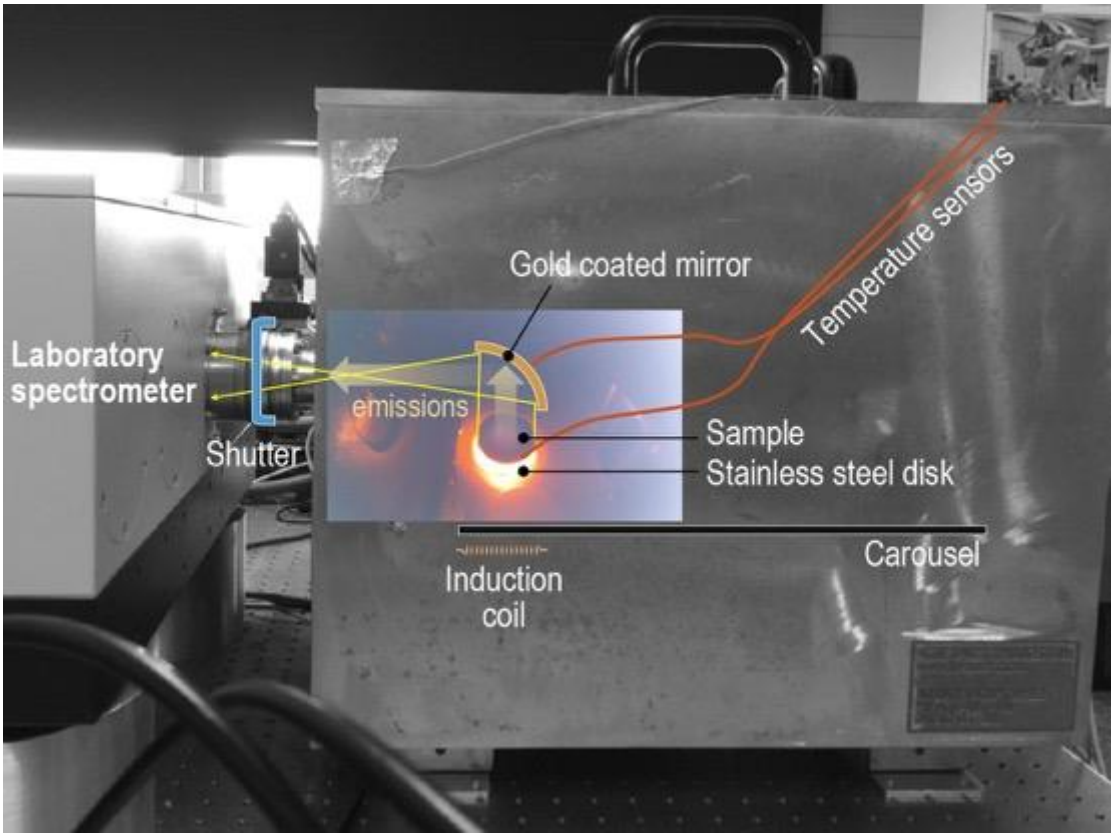

Figure 1. Graphical illustration of the laboratory set-up at PSL for high temperature emissivity measurements. The figure shows the heating of the sample cup using induction coil and its corresponding emissions been deflected to the Bruker 80V spectrometer using a gold-coated mirror. The image from inside the chamber was taken by a webcam during the measurement. The samples are placed in a stainless-steel disk,

which is then placed on the carousel. The induction coil heats the sample cup through the carousel. The shutter between the spectrometer and the emissivity chamber enables us to physically detach the emissivity chamber and spectrometer while heating under vacuum and therefore protecting the spectrometer from continuous heat emissions. The shutter is open only while recording the measurements when sample cup reaches its desired temperatures.

In this study, the emissivity spectral measurements of CaS are conducted for four simulated Mercury days each. The simple graphical flowchart of the experimental procedure is shown in Fig. 2. The detailed step by step experimental procedure is explained below:

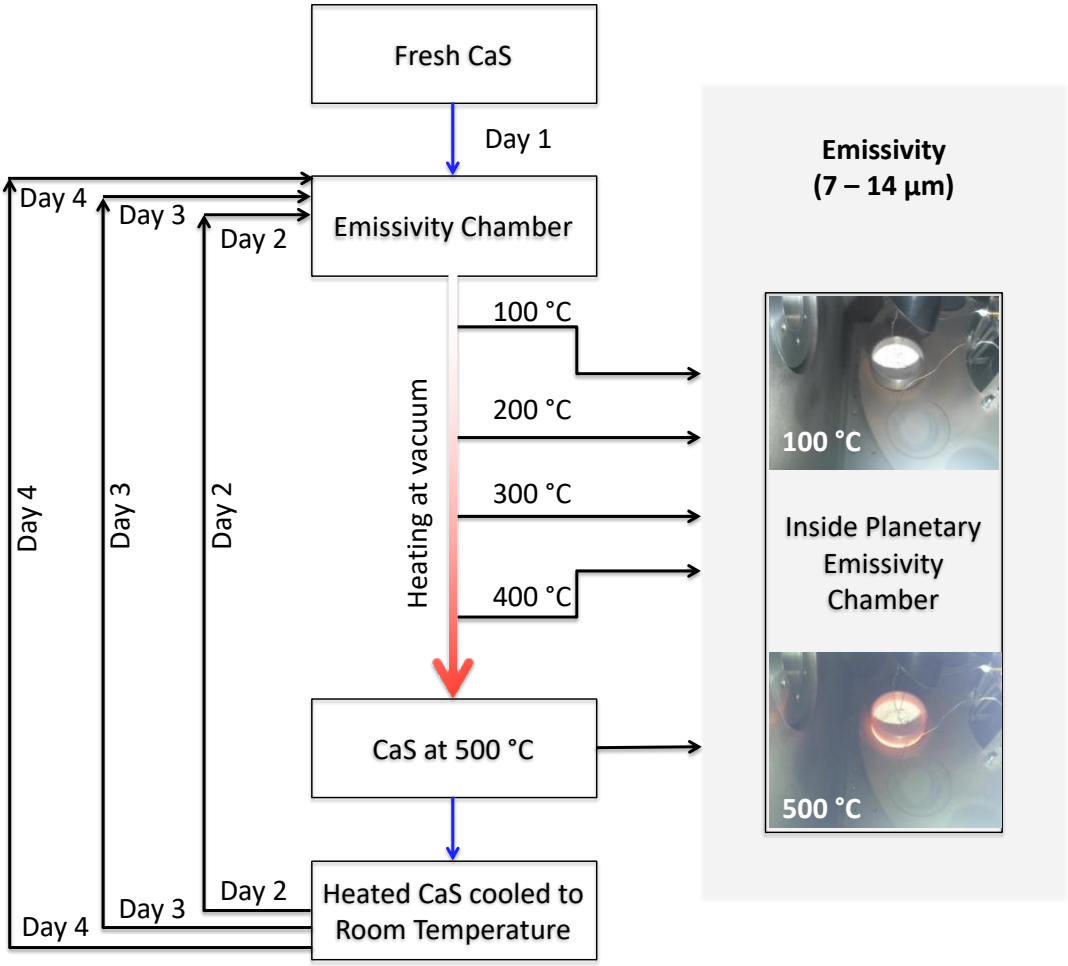

Figure 2. Graphical summary of the methodology used in the study to measure the emissivity of calcium sulfides (CaS) for four heating cycles during which the sample surface temperatures reach up to 500°C. The experimental set-up inside the emissivity chamber is also shown for temperatures 100 °C and 500 °C.

1. Once the experimental setup is ready and the fresh CaS sample loaded, both the spectrometer and the chamber are slowly evacuated. Before heating up, the sample is kept under vacuum for at least 1 hour to purge it from any air trapped in the sample. In the meantime, the detector is cooled down by liquid nitrogen.

2. Once the instrument and the chamber are stabilized under vacuum conditions, CaS is slowly heated up by manually controlling the current to the induction system. When the sample surface is stable at 100 °C, the first measurement takes place. The shutter between the chamber and the spectrometer opens, allowing the spectrometer to detect the radiance coming from the heated surface of CaS. The radiance is collected and deflected by a gold (Au) coated parabolic mirror at 90° off-axis into the spectrometer. After the measurement, the shutter is closed again to avoid that any particle reaches the spectrometer optics during heating process.

3. This procedure is repeated at temperatures of 200 °C, 300 °C, 400 °C, and 500 °C, thus obtaining the emissivity measurements for 1st simulated Mercury day.

4. After the last measurement at 500 °C, the chamber and the thermally processed CaS sample cool down overnight reaching room temperature. The vacuum condition is kept constant during the entire process. During the entire heating period, the CaS sample cup is never moved and is carefully monitored with the webcam installed in the chamber to detect outgassing events.

5. Each step from 2 to 4 is repeated every day for another three consecutive Earth days simulating a Mercury day cycle where the surface reaches up to 500 °C. For all the four days of measurements, the vacuum pump is continuously operated. The samples are therefore not exposed to the atmosphere during the entire experiment (Fig. 2).

At the end of the measurements, the CaS sample used for the measurements is by all means thermally processed (T-processed) under Mercury daytime temperatures. All the measured emissivity spectra of CaS, which are shown in Figure 3, are finally calibrated against a blackbody reference at their respective measured temperatures and geometric configurations. PSL uses blast furnace slag as a standard blackbody for the temperatures and spectral range used in this study (Maturilli et al., 2013).

2.2 X-Ray Diffraction (XRD)

In order to understand the physical stability of CaS under the extreme thermal environment of Mercury and to explain the observed changes in its spectral characteristics (Fig. 3), the XRD analyses of the fresh starting material (CaS) and the recovered thermally processed CaS were conducted at the Helmholtz Centre Potsdam - GFZ German Research Centre for Geosciences, Potsdam. The instrument used for the XRD analyses is a STOE STADI P powder diffractometer. The primary Cu $K_{\alpha 1}$ radiation was produced with 40 kV acceleration voltage and 40 mA beam current and a Ge (111) primary monochromator. The diffracted radiation was detected by a high-resolution DECTRIS MYTHEN detector. Measurements were performed in the range $2\theta = 5°\text{-}100°$ where 2θ is the angle between incident X-ray beam and reflected X-ray beam. The accuracy of the system was monitored before each measurement by collecting a full X-ray diffraction spectrum of Si standard (NIST 640d). The average value of the unit-cell parameter of Si is 5.430 ± 0.001 Å, which, compared to the certified value $a_0 = 5.43123 \pm 0.00008$ Å, corresponds to an accuracy of 0.02%.

The results obtained from the XRD measurements for starting and thermally processed CaS are shown in Fig. 4a and Fig. 4b respectively and are discussed in detail in Section 3.2

3. Results and Discussions

3.1 Emissivity measurements

The spectral evolution of calibrated emissivity of the CaS for four simulated Mercury days is discussed below:

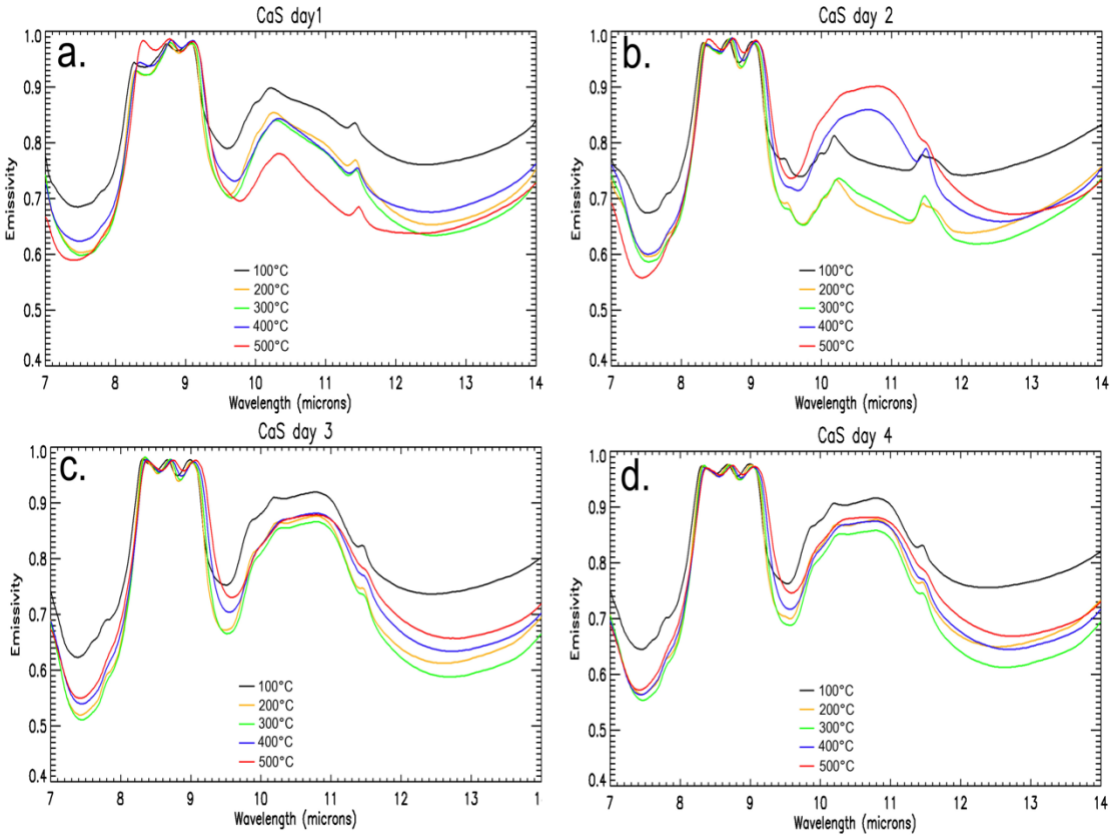

Figure 3. (a-d) Emissivity measurements showing emissivity behavior of CaS under four simulated Mercury daytime surface conditions where peak surface temperatures reach upto 400-500°C. (b) The evolution of an emissivity feature near 10-11 μm is observed for samples heated to >400 °C during second simulated Mercury day. (c-d) However, the spectra remained constant during the third and fourth day.

Simulated Mercury Day 1: With the increase of temperature from 100 to 500 °C during the first simulated Mercury day (Fig. 3a). We observed that: a) The band center near 7.5 μm remains constant until the sample reaches 400 °C, dropping shortwards to ~7.4 μm at 500 °C; b) The emissivity shows a maximum doublet near 8.8 μm and this spectral feature does not change in strength and position when heating from

100 °C to 400 °C, whereas at 500 °C, the emissivity near the 8.3 μm spectral shoulder slightly increases; c) The band center near 9.6 μm does not change until heating up to 300 °C but slightly shifts to longer wavelengths with increasing temperatures from 300 °C to 500 °C; d) The center of the spectral shoulder near 10.2 μm and the spectral spike near 11.4 μm slightly increase with increasing temperatures from 100 °C to 500 °C; and e) The emissivity for spectral features near 7.5 μm and 9.5 μm decreases with increasing temperatures.

Simulated Mercury Day 2: Emissivity spectra of CaS at 100 °C (Fig. 3b; black) during Day 2 show comparatively similar spectral shapes compared to emissivity spectra of CaS at 500 °C of Day 1 (Fig. 3a; red). Within the spectral region of 7.5-9.5 μm, the overall spectral morphology remains stable while heating up to 500 °C. However, the spectral shape at wavelength larger than 12 μm changes drastically when the sample temperature exceeds 400 °C. Up to 300 °C, the spectral shape between 10 μm and 12 μm display a negative slope having spectral shoulders (minor peaks in emissivity) at 10.2 μm and 11.4 μm. However, at temperatures 400 °C, this spectral slope evolves into a broad emissivity band. This spectral feature is also observed in spectra taken at 500 °C with a slight increase in emissivity.

Simulated Mercury Day 3: In order to test the stability of the emissivity spectra of CaS at the end of the measurements at Day 2 (Fig.3b; red), the emissivity procedure is repeated again for Day 3. At temperature of 100 °C (Fig. 3c; black) during Day 3, the emissivity of CaS maintains the spectral shape of CaS at 400 °C and 500 °C during the previous day (Fig. 3b; red). While heating through 200°, 300°, 400°, and 500°C, the general spectral morphology of the emissivity behavior of CaS did not show any significant changes. For all temperatures, a) the emissivity of CaS during Day 3 shows minima at ~7.5 μm and 9.5 μm, b) the emissivity maximum shows a doublet feature

centered around ~8.8 μm, and c) the spectral shape between 10 and 12 μm feature shows a broad spectral band in contrast to the spectral shape of Day 1.

Simulated Mercury Day 4: When the sample was heated again through the fourth simulated Mercury day (100-500 °C) under vacuum, the emissivity spectra remained unchanged with respect to the previous day (Day 3) at all respective temperatures.

At the end of the four days of emissivity measurements of the CaS sample under vacuum, a mild "rotten egg" odor was sensed while opening the chamber. This may indicate the release of S during the experiments.

3.2 XRD Analysis

In order to explain the changes in spectral characteristics of fresh CaS and the products after four heating cycles (Fig. 3), XRD analyses were conducted for the fresh starting CaS (corresponding to emissivity spectra during Day 1) and the resulting thermally processed CaS (corresponding to emissivity spectra during Day 4).

The measured XRD diffractogram of the starting/fresh CaS against the theoretical XRD diffractogram of pure CaS is plotted in Fig. 4a. The measured XRD diffractogram of our fresh CaS displays an extra peak (d-spacing at circa 1.35 Å) marked as red arrow in Fig. 4a which does not belong to the calculated XRD pattern of pure CaS. This extra peak is probably due to minor impurities in the starting material of the synthetic CaS sample. Hence, the emissivity spectra of CaS at all temperatures for Day 1 (Fig. 3a) does not correspond to the emissivity spectra of pure CaS.

However, this extra peak (d-spacing at circa 1.35 Angstrom) disappeared in the measured XRD pattern of the thermally processed (T-processed) CaS, which matches with all the peaks attributed to the calculated XRD pattern of pure CaS as shown in Fig. 4b. This disappearance of the extra peak in the T-processed CaS can be explained as,

impurities within the starting sample that either become amorphous or cryptocrystalline or even sublimated in the process of repeated heating up to 500 °C (Fig 4b). The match of the peaks of the measured XRD pattern of the thermally processed sample with the calculated XRD pattern of pure CaS (shown in Fig. 4b) confirms the thermal stability of CaS. Hence, the emissivity spectra of CaS at Day 4 at all temperatures correspond to the emissivity spectrum of pure CaS which is stable at even the extreme temperatures of Mercury and during repeated heating cycles.

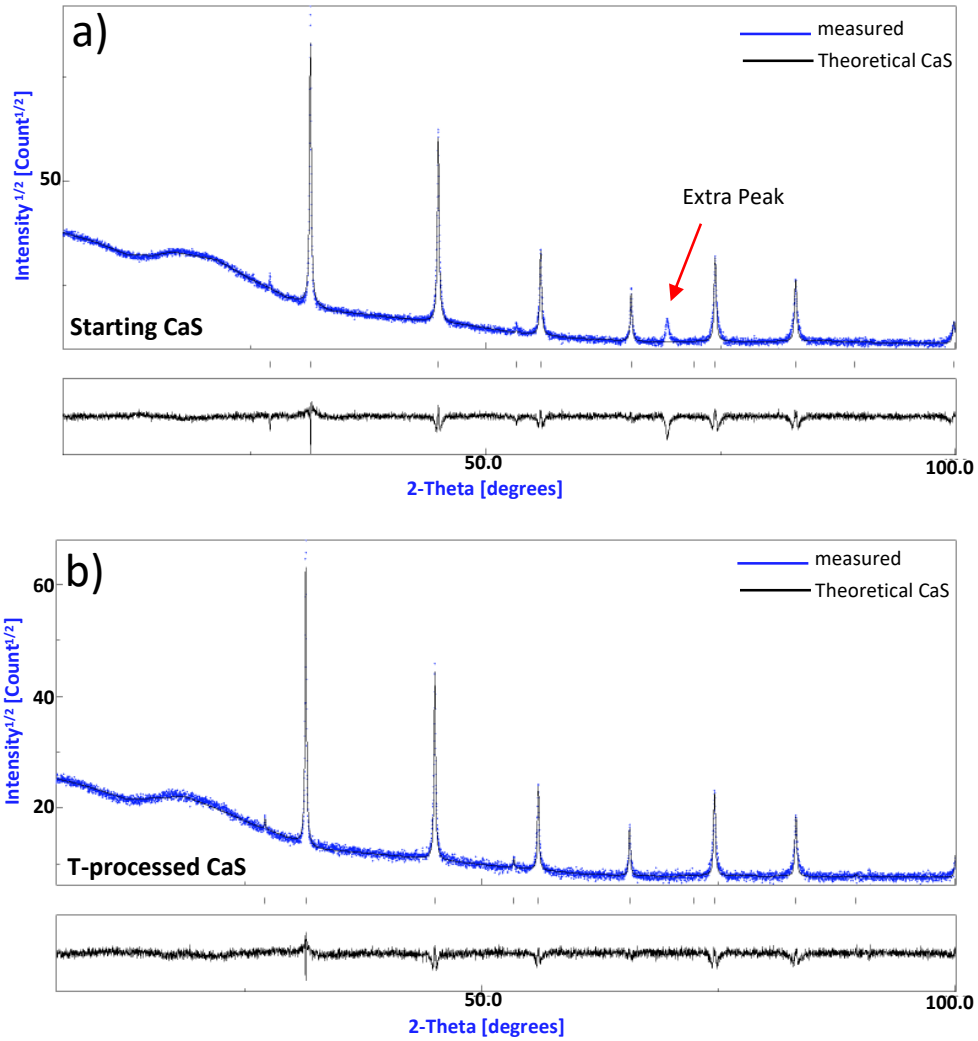

Figure 4. The XRD diffratogram results obtained for (a) fresh CaS and (b) thermally processed CaS after four heating cycles. The top plot for both (a) and (b) compares the measured (blue-dotted) and calculated XRD pattern of CaS (black solid). The bottom plot for both (a) and (b) shows the difference between observed and calculated XRD amplitudes of CaS. The presence of impurities in the starting/fresh CaS sample is indicated by the extra peak (d-spacing at circa 1.35 Angstrom) in the measured XRD

pattern of the starting sample in (a) marked by red arrow. This extra peak (d-spacing at circa 1.35 Angstrom) disappeared in the measured XRD pattern of the thermally processed CaS in (b) which could suggest that these impurities get amorphous or cryptocrystalline or even sublimated after heating upto 500 °C.

4. Implications

Several studies (Blewett et al., 2013; Helbert et al., 2013a) suggested that the formation of hollows can be attributed to the thermal decomposition/sublimation of volatile-rich minerals such as sulfides constituting the hollow materials. (Thomas et al., 2014a) conducted a global investigation of hollows on Mercury for its extent and size in order to understand their formation mechanism. The study showed that the hollows in the northern hemisphere are preferentially on sun-facing slopes implying a formation mechanism related to solar heating.

The emissivity of sulfides (7-14 μm) as a function of temperature under simulated Mercury daytime surface conditions showed that most of the proposed sulfides (MgS, FeS, CrS, TiS, NaS, and MnS) show spectrally evolving emissivity behavior changes with increasing surface temperatures (Varatharajan et al., 2019). This further suggests that these sulfides thermally decompose and sublimate when exposed to extreme thermal environment of Mercury, and probably form hollows.

Previous studies show that Mercury's 2:3 orbital resonance has a significant impact on the latitudinal and longitudinal dependence on the peak surface temperatures during Mercury days (Bauch et al., 2021; Krotikov and Shchuko, 1975; Soter and Ulrichs, 1967; Vasavada et al., 1999). Therefore, it is important to understand the maximum daytime temperature distribution of Mercury along with the spatial distribution of hollows for their effective mapping and detection (Helbert et al., 2013a; Vilas et al., 2016). In order to achieve this, we re-created the modeled temperature map

of Mercury derived from Bauch et al. (2021) which was mapped for Mercury latitudes between 60 °N and 60 °S and we overlaid the globally mapped hollow groups of Thomas et al. (2014a) (Fig. 5). The locations of hollow groups are re-mapped from the supplementary file provided in Thomas et al. (2014a). Both surface temperature and hollow distribution are overlaid on the MESSENGER MDIS Map Projected Low-Incidence Angle Basemap (LOI) of global monochrome map (750 nm) at a resolution of 256 pixels per degree (~166 m/pix) (Denevi et al., 2018; Hawkins et al., 2007) (Fig. 5).

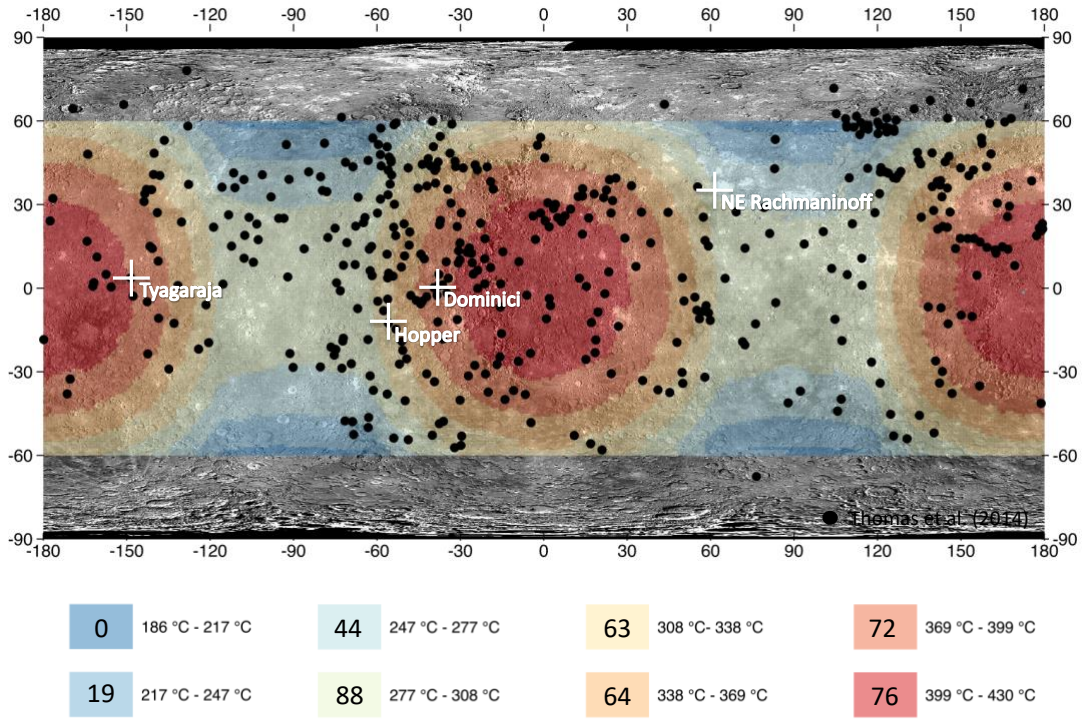

Figure 5. The peak surface temperature distribution across Mercury surface is mapped from (Bauch et al., 2021). The surface temperatures are overlaid on the MESSENGER MDIS global Map Projected Low-Incidence Angle Basemap (LOI) data set consists of a global monochrome map (750 nm) of reflectance at a resolution of 256 pixels per degree (~166 m/pix) (Denevi et al., 2018; Hawkins et al., 2007). The black datapoints indicate the distribution of hollows across Mercury's surface mapped by Thomas et al. (2014). The hollows within the Tyagaraja (3.89°N, 328.9°E), Dominici (1.38°N, 323.5°E), and Hopper (12.4°S 304.1°E) craters and NE Rachmaninoff (27.6°N, 57.4°E) are marked by white crosses.

Fig. 5 shows that hollows are distributed globally irrespective of the varying peak surface temperatures (T_{peak}). The total number of hollows in regions between 60 °N and 60 °S with peak daytime surface temperatures above ~300 °C (orange to red; Fig. 5) and below ~300 °C (blue to yellow; Fig. 5) are 275 and 151 respectively. Some notable examples are volcanic materials within the NE Rachmaninoff basin (27.6 °N, 57.4 °E) which are located within the temperature regime ~277 °C < T_{peak} <~308 °C (light green) whereas hollows within the Tyagaraja (3.89 °N, 328.9 °E) and Dominici (1.38 °N, 323.5 °E) craters are located in areas within ~369 °C < T_{peak}<~399 °C (intermediate red). Hopper (12.4 °S, 304.1 °E) crater is located within the temperature regime ~308 °C< T_{peak}<~338 °C (yellow) in Fig. 5. This compels the need for study for creating unique spectral library of various hollow-forming materials such as sulfides as a function of varying surface temperatures of Mercury (Varatharajan et al., 2019).

CaS belongs to the group of proposed sulfides of Mercury that constitute the chemical composition of surface features of presumably volcanic origin – such as hollow-forming minerals and pyroclastics (Besse et al., 2020; Helbert et al., 2013a; Vilas et al., 2016). In volcanic terrains, CaS has been proposed and spectrally detected in the hollows in visible-infrared spectral region using the MDIS data (Helbert et al., 2013a; Vilas et al., 2016). Varatharajan et al. (2019) demonstrated that most sulfides (MgS, FeS, CrS, TiS, NaS, and MnS) except for CaS are both physically and spectrally unstable when exposed to extreme daytime thermal environment of Mercury. The results from our study where CaS is exposed to repeated heating cycles under simulated Mercury daytime surface conditions (up to 500 °C), strongly suggest that CaS is the most stable sulfide against thermal weathering on Mercury's surface. This indirectly suggests that unlike other sulfides (MgS, FeS, CrS, TiS, NaS, and MnS), CaS may not significantly contribute to hollow formation on Mercury by solar heating as CaS does

not decompose with repeated heating cycles even under extreme temperatures reaching up to 500 °C. This would make CaS (if detected and mapped by MERTIS) a good tracer for sulfides (possibly among other volatiles) on Mercury that leads to formation of hollows, as other sulfides are lost in sublimation leaving behind the hollows.

In fact, CaS was successfully detected within the hollows of Dominici and Hopper craters (Vilas et al., 2016) and these craters occur in surface regions where peak temperatures reach ~400 °C as marked in Fig. 5. Future studies that combine the global mapping of CaS, the extent and depth of hollows bearing CaS and other sulfides will give further insight into the nature of volatiles on Mercury's surface and its interior as well as hollow forming mechanisms. As the emissivity behavior of pure CaS does not evolve with increasing surface temperatures, CaS can be globally mapped irrespective of the peak surface temperatures/heating cycles across Mercury.

Furthermore, the spectral investigation of various sulfides by Varatharajan et al. (2019) showed that the TIR spectral region is sensitive for the detection and characterization of sulfide minerals under Mercury daytime conditions. Hence, MERTIS onboard the BepiColombo mission will support the global mapping of volatiles on Mercury's surface and will help understanding the hollow forming mechanisms and its materials. Ultimately, such studies will help calculating the volatile budget of Mercury's interior and its contributions to Mercury's exosphere.

5. Conclusions

In this study, the physical and spectral stability of CaS has been investigated for four simulated Mercury days (heating cycles). The study indicates that calcium sulfide (CaS) is stable on Mercury's surface with emissivity spectra retaining their characteristic features irrespective of surface temperatures and repeated heating cycles

typical for Mercury. At all surface temperatures, the presence of CaS on Mercury surface can be identified by its emissivity behavior in the TIR spectral region (7-14 μm) which is characterized by a) a spectral minimum at ~7.5 μm and 9.5 μm, b) an emissivity maximum centered around ~8.8 μm with a peak doublet, and c) a broad spectral band between 10 and 12 μm. Our study demonstrates that CaS is the least thermally weathered sulfide among those expected on Mercury's surface, making it a good tracer for the presence of sulfides (possibly among other volatiles) associated with hollows and pyroclastics when globally mapped by MERTIS. The unique spectral library provided with this work will support global mapping of CaS around hollows and pyroclastic materials of Mercury surface using MERTIS payload onboard BepiColombo mission. The global mapping of CaS along with other sulfides across hollows will further help our understanding of the hollow formation mechanism dominated by sublimation process.

Acknowledgements

IV thank DLR/DAAD Doctorate Fellowship for funding her PhD work at PSL-DLR. A portion of this research was supported by the European Union's Horizon 2020 research and innovation program. Europlanet 2020 RI has received funding from the European Union's Horizon 2020 research and innovation programme under grant agreement No 654208.

References

Bauch, K.E., Hiesinger, H., Greenhagen, B.T., Helbert, J., 2021. Estimation of surface temperatures on Mercury in preparation of the MERTIS experiment onboard BepiColombo. Icarus 354, 114083.

Besse, S., Doressoundiram, A., Barraud, O., Griton, L., Cornet, T., Muñoz, C., Varatharajan, I., Helbert, J., 2020. Spectral Properties and Physical Extent of Pyroclastic Deposits on Mercury: Variability Within Selected Deposits and Implications for Explosive Volcanism. Journal of Geophysical Research: Planets 125, e2018JE005879.

Blewett, D.T., Vaughan, W.M., Xiao, Z., Chabot, N.L., Denevi, B.W., Ernst, C.M., Helbert, J., D'Amore, M., Maturilli, A., Head, J.W., Solomon, S.C., 2013. Mercury's hollows: Constraints on formation and composition from analysis of geological setting and spectral reflectance. Journal of Geophysical Research: Planets 118, 1013-1032.

Denevi, B.W., Chabot, N.L., Murchie, S.L., Becker, K.J., Blewett, D.T., Domingue, D.L., Ernst, C.M., Hash, C.D., Hawkins, S.E., III, Keller, M.R., Laslo, N.R., Nair, H., Robinson, M.S., Seelos, F.P., Stephens, G.K., Turner, F.S., Solomon, S.C., 2018. Calibration, Projection, and Final Image Products of MESSENGER's Mercury Dual Imaging System. Space Science Reviews 214.

Hawkins, S.E., Boldt, J.D., Darlington, E.H., Espiritu, R., Gold, R.E., Gotwols, B., Grey, M.P., Hash, C.D., Hayes, J.R., Jaskulek, S.E., 2007. The Mercury dual imaging system on the MESSENGER spacecraft. Space Science Reviews 131, 247-338.

Helbert, J., Dyar, D., Maturilli, A., Widemann, T., Marcq, E., Rosas-Ortiz, Y., Walter, i., D'Amore, M., Alemanno, G., Mueller, N., Smrekar, S., 2019. Spectroscopy

437 of the Surface of Venus - in the Laboratory and from Orbit, EPSC-DPS Joint
438 Meeting 2019.

439 Helbert, J., Maturilli, A., 2009. The emissivity of a fine-grained labradorite sample at
440 typical Mercury dayside temperatures. Earth and Planetary Science Letters 285,
441 347-354.

442 Helbert, J., Maturilli, A., D'Amore, M., 2013a. Visible and near-infrared reflectance
443 spectra of thermally processed synthetic sulfides as a potential analog for the
444 hollow forming materials on Mercury. Earth and Planetary Science Letters 369–
445 370, 233-238.

446 Helbert, J., Nestola, F., Ferrari, S., Maturilli, A., Massironi, M., Redhammer, G.J.,
447 Capria, M.T., Carli, C., Capaccioni, F., Bruno, M., 2013b. Olivine thermal
448 emissivity under extreme temperature ranges: Implication for Mercury surface.
449 Earth and Planetary Science Letters 371–372, 252-257.

450 Hiesinger, H., Helbert, J., Alemanno, G., Bauch, K.E., D'Amore, M., Maturilli, A.,
451 Morlok, A., Reitze, M.P., Stangarone, C., Stojic, A.N., Varatharajan, I., Weber,
452 I., the, M.C.-I.T., 2020. Studying the Composition and Mineralogy of the
453 Hermean Surface with the Mercury Radiometer and Thermal Infrared
454 Spectrometer (MERTIS) for the BepiColombo Mission: An Update. Space
455 Science Reviews 216, 110.

456 Hiesinger, H., Helbert, J., MERTIS Co-I Team, 2010. The Mercury Radiometer and
457 Thermal Infrared Spectrometer (MERTIS) for the BepiColombo mission.
458 Planetary and Space Science 58, 144-165.

459 Krotikov, V., Shchuko, O., 1975. Thermal conditions in the surface layer of Mercury.
460 Soviet Astronomy 19, 86-89.

461 Lucchetti, A., Pajola, M., Galluzzi, V., Giacomini, L., Carli, C., Cremonese, G., Marzo,
462 G.A., Ferrari, S., Massironi, M., Palumbo, P., 2018. Mercury Hollows as
463 Remnants of Original Bedrock Materials and Devolatilization Processes: A
464 Spectral Clustering and Geomorphological Analysis. Journal of Geophysical
465 Research: Planets 123, 2365-2379.

466 Maturilli, A., Donaldson Hanna, K.L., Helbert, J.r., Pieters, C., 2013. A New Standard
467 for Calibration of High Temperature Emissivity: Laboratory Intercalibration at
468 PEL of DLR and ALEC of Brown University, LPSC 2013.

469 Maturilli, A., Helbert, J., Moroz, L., 2008. The Berlin emissivity database (BED).
470 Planetary and Space Science 56, 420-425.

471 Nittler, L.R., Starr, R.D., Weider, S.Z., McCoy, T.J., Boynton, W.V., Ebel, D.S., Ernst,
472 C.M., Evans, L.G., Goldsten, J.O., Hamara, D.K., Lawrence, D.J., McNutt,
473 R.L., Schlemm, C.E., Solomon, S.C., Sprague, A.L., 2011. The Major-Element
474 Composition of Mercury's Surface from MESSENGER X-ray Spectrometry.
475 Science 333, 1847-1850.

476 Soter, S., Ulrichs, J., 1967. Rotation and Heating of the Planet Mercury. Nature 214,
477 1315-1316.

478 Thomas, R.J., Rothery, D.A., Conway, S.J., Anand, M., 2014a. Hollows on Mercury:
479 Materials and mechanisms involved in their formation. Icarus 229, 221-235.

480 Thomas, R.J., Rothery, D.A., Conway, S.J., Anand, M., 2014b. Long-lived explosive
481 volcanism on Mercury. Geophysical Research Letters 41, 6084-6092.

482 Varatharajan, I., Maturilli, A., Helbert, J., Alemanno, G., Hiesinger, H., 2019. Spectral
483 behavior of sulfides in simulated daytime surface conditions of Mercury:
484 Supporting past (MESSENGER) and future missions (BepiColombo). Earth
485 and Planetary Science Letters 520, 127-140.

486 Vasavada, A.R., Paige, D.A., Wood, S.E., 1999. Near-Surface Temperatures on
487 Mercury and the Moon and the Stability of Polar Ice Deposits. Icarus 141, 179-
488 193.

489 Vaughan, W.M.H., J. W.; Parman, S. W.; Helbert, J. , 2013. What Sulfides Exist on
490 Mercury? 44th Lunar and Planetary Science Conference 2013.

491 Vilas, F., Domingue, D.L., Helbert, J., D'Amore, M., Maturilli, A., Klima, R.L.,
492 Stockstill-Cahill, K.R., Murchie, S.L., Izenberg, N.R., Blewett, D.T., Vaughan,
493 W.M., Head, J.W., 2016. Mineralogical indicators of Mercury's hollows
494 composition in MESSENGER color observations. Geophysical Research
495 Letters 43, 1450-1456.

Weider, S.Z., Nittler, L.R., Murchie, S.L., Peplowski, P.N., McCoy, T.J., Kerber, L., Klimczak, C., Ernst, C.M., Goudge, T.A., Starr, R.D., Izenberg, N.R., Klima, R.L., Solomon, S.C., 2016. Evidence from MESSENGER for sulfur- and carbon-driven explosive volcanism on Mercury. Geophysical Research Letters 43, 3653-3661.

Weider, S.Z., Nittler, L.R., Starr, R.D., McCoy, T.J., Solomon, S.C., 2014. Variations in the abundance of iron on Mercury's surface from MESSENGER X-Ray Spectrometer observations. Icarus 235, 170-186.

Weider, S.Z., Nittler, L.R., Starr, R.D., McCoy, T.J., Stockstill-Cahill, K.R., Byrne, P.K., Denevi, B.W., Head, J.W., Solomon, S.C., 2012. Chemical heterogeneity on Mercury's surface revealed by the MESSENGER X-Ray Spectrometer. Journal of Geophysical Research: Planets 117, n/a-n/a.